

Energy Separation in a Counter-Flow Vortex Tube: An Experimental Study and CFD Analysis

Lizan Mahmood Khorsheed Zangana^{*,**} and Ramzi Raphael Ibraheem Barwari^{**}

Keywords : Vortex Tube, CFD Analysis, Experimental Study, Energy Separation.

ABSTRACT

In this manuscript, both experimental and numerical investigations have been carried out to study the mechanism of separation energy and flow phenomena in the counter-flow vortex tube. This manuscript presents a complete comparison between the experimental investigation and CFD analysis. The experimental model tested under different inlet pressures. 3D numerical modelling using the $k-\epsilon$ model used with code (Fluent 6.3.26). The results show any increase in both cold mass fraction and inlet pressure caused to increase ΔT_c , and the maximum ΔT_c value occurs at $P = 6$ bar. The coefficient of performance (COP) of two important factors which are a heat pump and a refrigerator have been evaluated, which ranged from 0.25 to 0.74. The maximum axial velocity is 93, where it occurs at the tube axis close to the inlet exit ($Z/L=0.2$). The results showed a good agreement for experimental and numerical analysis.

INTRODUCTION

The essential use of thermodynamics is refrigeration, in this process, it can be considered the heat is transferred from the low-temperature region to the high-temperature region with the working fluid named "refrigerant" (Dawoodian et al. 2014). One of the non-conventional systems where natural matter such as air is used as a working medium is the vortex tube (Pourmahmoud et al. 2015a).

Paper Received September, 2019. Revised January, 2020. Accepted January, 2020. Author for Correspondence: Lizan Mahmood Khorsheed Zangana

** Department of Petroleum Equipment, Erbil Technology Institute, Erbil Polytechnic University, Kirkuk Road, Hadi Chawshli Street, Erbil, Iraq*

***Mechanics and Mechatronics Department, College of Engineering, Salahaddin University-Erbil, Kirkuk Street Road, Erbil, Iraq.*

with more in some designs, a vortex chamber, a cold-end orifice diameter, a hot-end control valve. The history of the vortex tube returns to early in the twentieth century, where George Ranque was proposing a study about a vortex tube in the subject of dust separation cyclone George J. Ranque (1933). After that R. Hilsch examined the influence of the geometrical parameters and the inlet pressure of the vortex tube (Hilsch 1947). The vortex tube has high inefficient thermodynamically characteristics, which used in the cooling of gas turbine rotor blades, laboratory sample cooler, cooling electrical cabinets (Pourmahmoud et al. 2013 and 2014a). Vortex tube splits up a pressurized flow of air into two streams hot and cold. In the vortex tube, the air is compressed tangentially, where it separates into two lower pressure streams; the external, and the internal. The phenomenon of the vortex tube is shown in Fig. 1.

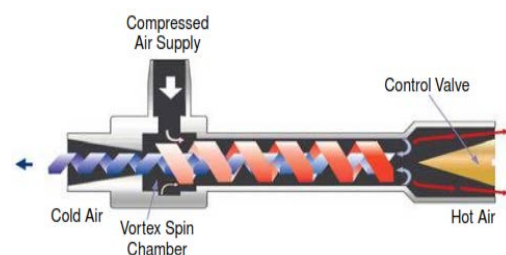


Fig. 1. Schematic of Vortex tube behavior (Pourmahmoud et al. (2015b))

The phenomenon mechanism of the temperature separation accordingly to state gas or vapour come back to a Ranque-Hilsch vortex tube is not completely understood until now due to complexity, although various investigators lay many efforts to demonstrate the behavior happening through the separation of energy in the vortex tube. They focused on the geometrical and thermophysical in the

Experimental study work. Pourmahmoud et al. (2014b) estimate in numerical technique the influence of the inlet pressure to enhance the cooling capacity. Their CFD models used turbulent, compressible, and using the standard k- ϵ turbulence model.

Few researchers have been carried out to investigate the temperature separation for both Kalal et al. (2008) investigated both studies of the experimental and CFD analysis using the k- ϵ turbulence model on parameters affecting vortex tube operations length from (200- 1450 mm), cold end diameters (8, 10, 12 and 14 mm) and numbers of nozzles (2 and 4). The results showed that for a length of 1000 mm and the cold outlet diameter of 12 mm is optimum for the maximum temperature difference. Ye et al. (2014) investigated the energy separation in the vortex chamber in experimental and CFD analysis. The study showed the distribution of the angular momentum showed energy migration. Kirmaci and Kaya (2018) presented a review on the effect of various parameters such as working fluid, nozzle number, and nozzle material investigated by both experiments and simulation. From the invention vortex tube, various explanations were suggested for energy separation. However, because of the nature of the energy separation and complexity of internal flow in the vortex tube, the energy separation phenomenon until now is still unclear. In this paper, the study will include two methods, numerical study (CFD) and experimental investigation. Analysis and simulations are used to evaluate the presented theoretical fundamentals, the flow field in the vortex tube simulated numerically by using FLUENT™ software package simulation. The standard k- ϵ turbulence model applied to simulate the effect of turbulence in the vortex tube flow. The counterflow vortex tube has been designed to evaluate various parameters such as cold and hot exit temperatures, isentropic efficiency, cold mass fraction, and velocities. Using Simulation and experiments to ensure efficient operation of energy separation (temperature separation) over the entire operating range.

EXPERIMENTAL SETUP

In the present manuscript, an experimental investigation has been employed to estimate the influence of working fluid parameters like inlet pressure on the energy separation inside the vortex tube. In the present work, the counter-flow vortex tube has been designed, fabricated, and tested to evaluate various parameters such as cold and hot exit temperatures, refrigerating effect, and isentropic efficiency. Fig. 2 shows the experimental apparatus parts of the present counter-flow vortex tube and Fig. 3 illustrates the vortex tube parts used in this paper. The compressed air is supplied across compressor tank storage to ensure to get uniform pressure with

minimum variation. The tank storage has a capacity of 1000 liters, and the system is working approximately half an hour before running the test to allow system temperature to stabilize. The maximum rated pressure of the compressor is 6 bars with inlet pressure varied from (4-6 bars) and regulated by a pressure regulator the pressure gauge. The compressed air passed through a filter to clean air from particles and residuals to ensure to use of cleanly dry air. The vortex tube used counter-flow with six inlet nozzles, vortex chamber, cold orifice, hot side valve, cold and hot ends, as shown in the schematic diagram in Fig. 3.



Fig. 2. Experimental parts



Fig. 3. Parts of vortex Tube in the present study

The air is extended in the vortex chamber and split into the cold and hot air flows. The cold stream in the central region flows out of the tube through the center orifice nearby to the inlet nozzle, while the hot stream in the external annulus departs the tube across another outlet away from the inlet. The flow rate of the inlet air is adjusted with flow rates while the inlet and outlet temperatures of the streams are calculated with multiple thermometers. The schematic of the current vortex tube setup has been depicted in Fig. 4. The material used in the vortex tube is manufactured of stainless steel with an inner diameter and the length of the tube is 8 mm, 104 mm respectively. The outlet diameter of the cold side is 5.5 mm as shown in the geometrical design in Fig. 5. Since the present paper is experimental research, therefore, the uncertainties of measured and calculated temperatures have been displayed in figure 6.

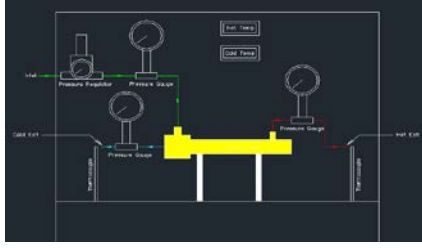


Fig. 4. Schematic diagram setup

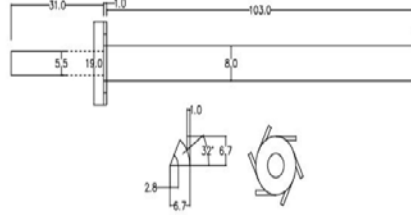


Fig. 5. 2D cross-section of the vortex tube.

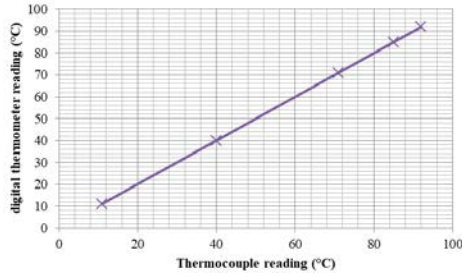


Fig. 6. Uncertainties measurement

NUMERICAL MODELING AND GOVERNING EQUATIONS

The rapid development of computational fluid dynamics (CFD) provides a convenient and faster way to study these variables in a vortex tube (Sadaghiyani et al. (2018), Khodayari and Kim (2018)). Numerical modeling is the most precise technique to study the phenomenon of the vortex tube. So it's necessary for the choice of a suitable turbulence model. The software is capable of solving a set of equations numerically by using numerical iteration techniques. The software is a powerful tool that can allow compiling multiple equations while allowing easy access to fluid properties (Matveev and Leachman, 2019). The numerical simulation of the flow field will be assumed by using the FLUENT software package. The equations are solved as consider the flow to be 3D compressible (Promvonge and Eiamsa-ard, 2005) and to solve the equation of continuity equation, momentum, and energy which are as follows:

Continuity equation:

$$\frac{\partial}{\partial x_j}(\rho u_j) = 0 \quad (1)$$

Momentum (the rate change of momentum) is the sum of the forces on the fluid particle (Newton's second law):

$$\frac{\partial}{\partial x_j}(\rho u_i u_j) = -\frac{\partial p}{\partial x_i} + \frac{\partial}{\partial x_j} \left[\mu \left(\frac{\partial u_i}{\partial x_j} + \frac{\partial u_j}{\partial x_i} - \frac{2}{3} \delta_{ij} \frac{\partial u_k}{\partial x_k} \right) \right] + \frac{\partial}{\partial x_j}(-\rho \overline{u_i u_j}) \quad (2)$$

Energy equation is equal to the sum of (rate of heat added to and the rate of work done) (1st law of thermodynamics):

$$\frac{\partial}{\partial x_i} \left[u_i \rho \left(h + \frac{1}{2} u_j u_j \right) \right] = \frac{\partial}{\partial x_j} \left[k_{eff} \frac{\partial T}{\partial x_j} + u_i (\tau_{ij})_{eff} \right],$$

$$k_{eff} = K + \frac{c_p \mu_t}{Pr_t} \quad (3)$$

The motion of the fluid in the vortex tube is described with the governing equations (mass, momentum, and energy conservation), so among unknown are three thermodynamic variables: ρ , p , and T . The relationships between the thermodynamics variables can be obtained through an assumption of the thermodynamic equilibrium. Even though the properties of fluid-particle change rapidly from place to place, the fluid can thermodynamically adjust itself to new conditions so quickly that changes are effectively instantaneous. So the state equations for pressure as following as:

$$p = \rho RT \quad (4)$$

The standard k- ϵ has two model equations:

$$\frac{\partial}{\partial t}(\rho k) + \frac{\partial}{\partial x_i}(\rho k u_i) = \frac{\partial}{\partial x_j} \left[\left(\mu + \frac{\mu_t}{\sigma_k} \right) \frac{\partial k}{\partial x_j} \right] + G_k + G_b - \rho \epsilon - Y_M \quad (5)$$

$$\frac{\partial}{\partial t}(\rho \epsilon) + \frac{\partial}{\partial x_i}(\rho \epsilon u_i) = \frac{\partial}{\partial x_j} \left[\left(\mu + \frac{\mu_t}{\sigma_\epsilon} \right) \frac{\partial \epsilon}{\partial x_j} \right] + C_{1\epsilon} \frac{\epsilon}{k} (G_k + C_{3\epsilon} G_b) - C_{2\epsilon} \rho \frac{\epsilon^2}{k} \quad (6)$$

$$\mu_t = \rho C_\mu \frac{k^2}{\epsilon} \quad (7)$$

VORTEX TUBE PHYSICAL MODELING

The CFD models of the present study are considered based on this new experimental analysis, 3D with a standard k- ϵ turbulence model will be investigated numerically under different geometrical parameters such as inlet pressure. As inlet air is assumed as a compressible so all these parameters are constant values (dynamic viscosity, specific heat, and thermal conductivity). To solve the momentum and energy equations, SIMPLE algorithm will be used

and due to non-linear and coupling virtue is very high of the governing equations, for the ρ , P , body forces, k , ϵ , and turbulent viscosity components, lower under-relaxation factors will take ranging from 0.1. To reduce the computations only 1/6 sector of the flow domain CFD model will be assumed. The 3D model shows in fig.7. To recognize the temperature distribution inside the vortex tube, fig. 8 shows the temperature contours in the longitudinal section for the chosen models

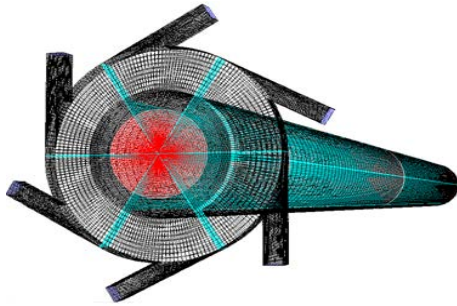


Fig. 7. 3D CFD Model of Vortex Tube

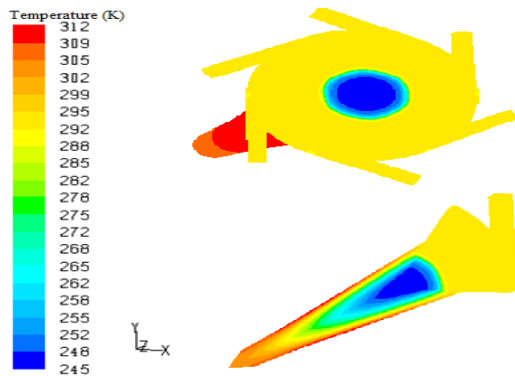


Fig. 8. Temp. distribution in longitudinal section for $P_i = 6$ bar and $\alpha = 0.3$

BOUNDARY CONDITION

The boundary conditions in this numerical work are based on the present experimental study, which mentioned above. At inlets of the nozzle, the air is compressed into the tube with inlet gas temperature (stagnation temperature) is fixed at 293 K, pressure inlet is varied from (4-6 bars), and the cold mass fraction 0.3 to 0.8. The pressure will be adjusted to vary with the cold mass fraction ant the hot outlet. The no-slip velocity boundary condition is enforced on all of the walls of the vortex tube, and it is assumed to be adiabatic.

RESULTS AND DISCUSSION

Comparison of CFD Results and Experimental Data for Temperature Separation

$$\alpha = \frac{\dot{m}_c}{\dot{m}_{in}} \tag{8}$$

Where \dot{m}_c and \dot{m}_{in} stand for cold and inlet mass flow rates, respectively. The cold and hot exit temperature differences (ΔT_c and ΔT_h , respectively) are defined as follows:

$$\Delta T_{i,c} = T_i - T_c \tag{9}$$

$$\Delta T_{h,i} = T_h - T_i \tag{10}$$

As below, Tables 1 and 2 show the experimental data and the CFD simulation, respectively. It can be noticed a good agreement between the results. It can be seen from the results, as the inlet pressure increases, the ΔT_c and ΔT_c increases, and a maximum value occurs at $P_i = 6$ bar. The CFD model and the experimental data Comparisons are shown in terms of the inlet pressure and the 3D CFD results can well predict the experimental results. In this investigation, CFD results close well with experimental data with a deviation of the predicted and measured data is less than or equal to 7.79% for the cold temperature difference.

Table 1. The experimental data at cold mass fraction 0.3

P_i (bar)	T_c (K)	T_h (K)	$\Delta T_{i,c}$ (K)	$\Delta T_{h,i}$ (K)
4	250.67	305.92	42.32	12.92
5	247.93	307.82	45.06	14.82
6	243.44	310.48	48.34	17.48

Table 2. The CFD results at cold mass fraction 0.3.

P_i (bar)	V_{sm} (m/s)	T_c (K)	T_h (K)	$\Delta T_{i,c}$ (K)	$\Delta T_{h,i}$ (K)
4	390	253.98	309.95	39.02	16.95
5	400	250.44	310.93	46.75	10
6	420	245.9	313.62	47.10	20.62

Numerical Results

To analyze the thermodynamical estimation of rate of energy (power) separation with another valuation as heating or cooling capacity of a vortex tube. Regarding as refrigerator gains as eq. (12) and a heat engine as eq. (13) by:

$$\dot{Q}_c = \dot{m}_c c_p (T_i - T_c) \quad (12)$$

$$\dot{Q}_h = \dot{m}_h c_p (T_h - T_i) \quad (13)$$

As shown in figures 9 and 10, \dot{Q}_c it is maximum for $\alpha = 0.65$ and \dot{Q}_h is maximum for $\alpha = 0.37$. The energy separation varies from 0.055 to 0.155 kW. It shows that in the vortex tube system, the essential goals must be focused on the use of this instrument in the heating or cooling process only; so that, the criteria of the classical thermodynamics would not be justified in various conditions. These results are in good agreement with those of Behera et al. (2005).

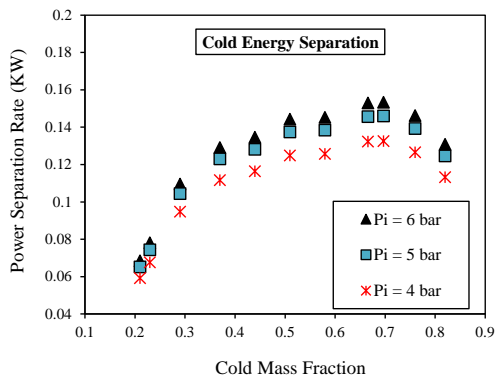


Fig. 9. Refrigeration power separation of the vortex tube with different nozzles.

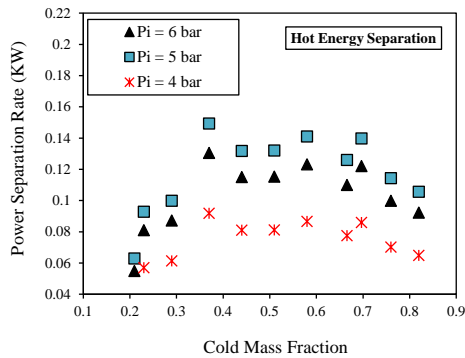
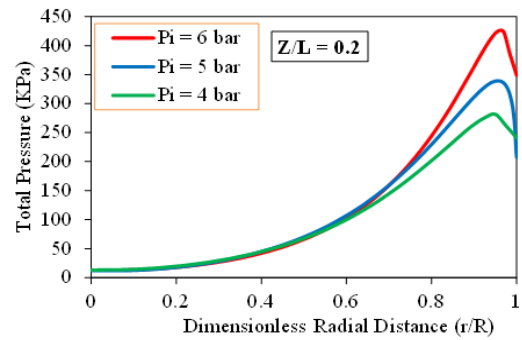


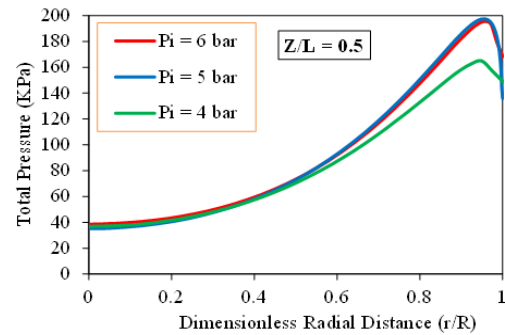
Fig. 10. Heat power separation of the vortex tube with different nozzles.

The large expansion happens at the end of the nozzle, which made a rise in velocity. Just after extract of the fluid across the nozzles to the tube. The gas extended again, upward to the cold exit, where it falls to atmospheric pressure, which causes rise velocity in this region. The highest total pressure noticed nearby the circumstance of the tube wall all simulated CFD models. The profiles of the total pressure appears a

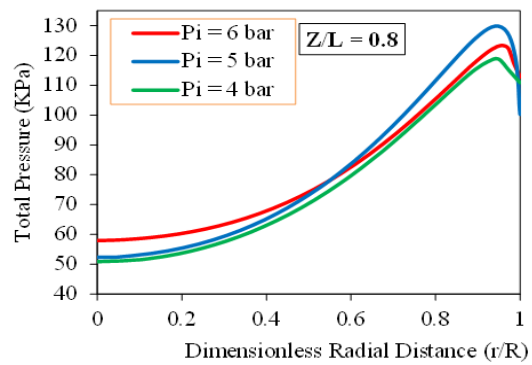
rise of the pressure magnitude in a portion of the wall. Both total and static pressures rise with increasing the inlet pressures as shown in Figs. 11 and 12.



(a)

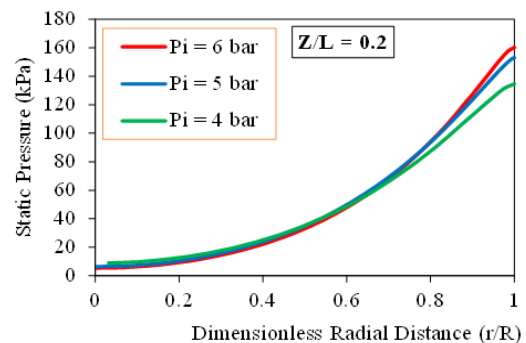


(b)



(c)

Fig. 11. Radial profiles of total pressure at different axial locations



(a)

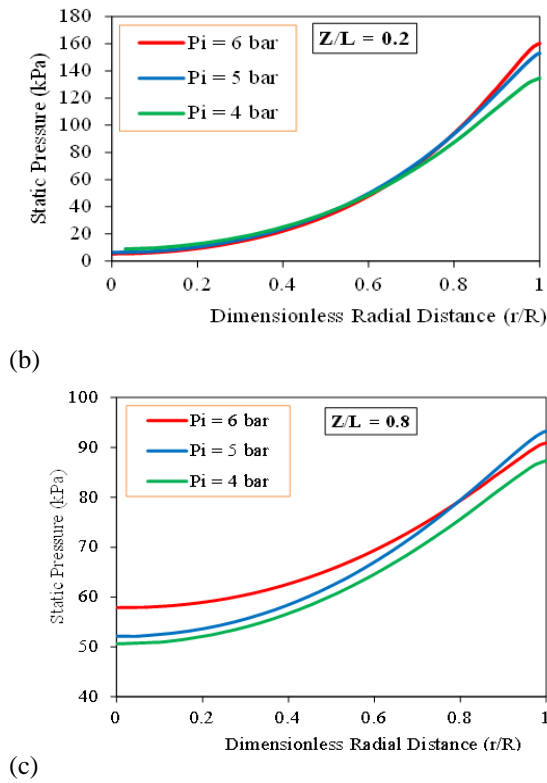


Fig. 12. Radial profiles of static pressure at different axial locations.

With changing the inlet pressure, radial profiles of swirl velocity at various axial locations ($Z/L = 0.2, 0.5,$ and 0.8) for the cold mass fraction of 0.3 to 0.8 are displayed in fig. 13. The comparison of the velocity, it is very noticeable that the component which has the highest value is a swirl velocity. The radial profile of the swirl velocity points out a free vortex near the wall, and the magnitude becomes negligibly small at the core. The flow near the injection of a vortex tube as a forced vortex can be expressed as:

$$\omega = \frac{v}{r} \tag{14}$$

Where v is the velocity of the flow particle and r is the radial distance from the centerline of the tube. In all models with any rise, the distance from the inlet region across the hot exit, the swirl velocity value came down. And in the core of the vortex tube, the fluid has a deficient kinetic energy result of the minimum swirl velocity at the core region of the tube. The radial profiles for the axial velocity at $Z/L=0.2, 0.5$ and 0.8 are shown in fig. 14. For the $P_i = 6$ bar at axial locations of $Z/L=0.2, 0.5$ and 0.8 the maximum axial velocity was noticed $83, 44$ and 41 m/s, respectively. Therefore, the highest range of 83 m/s is seen at the tube axis near the inlet zone ($Z/L=0.2$).

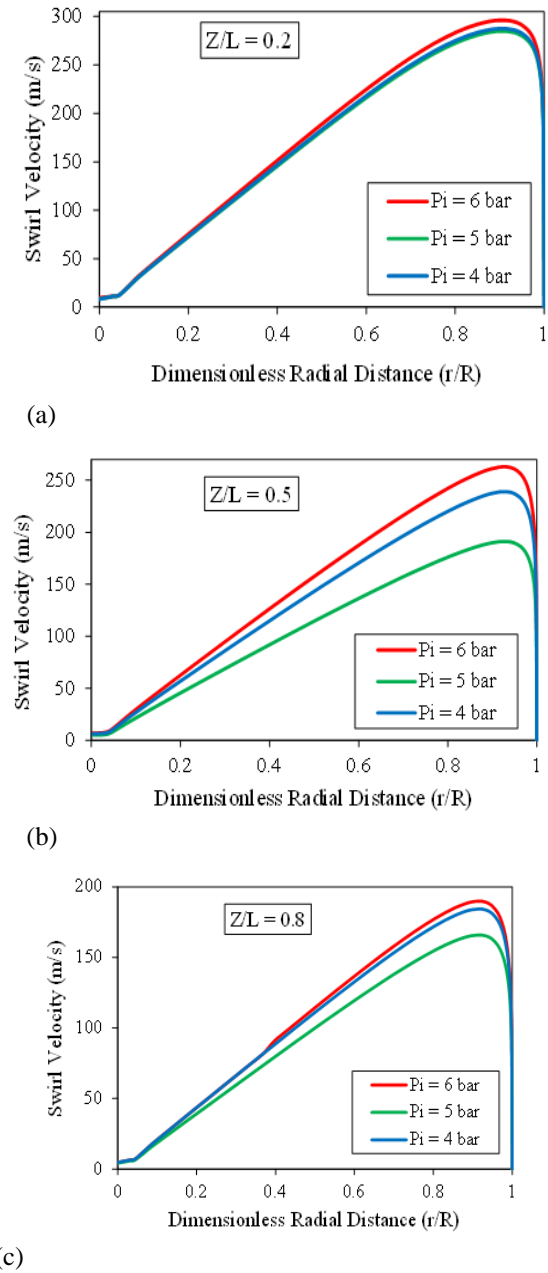
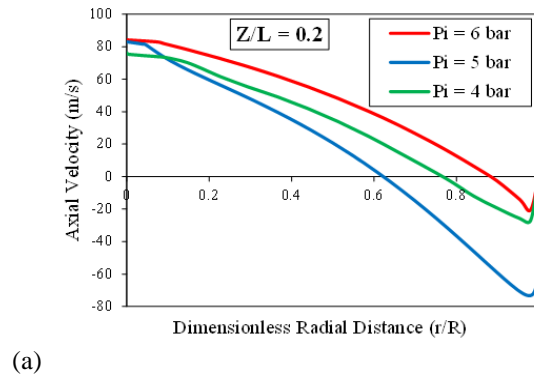


Fig. 13. Radial profiles of swirl velocity at different axial locations.



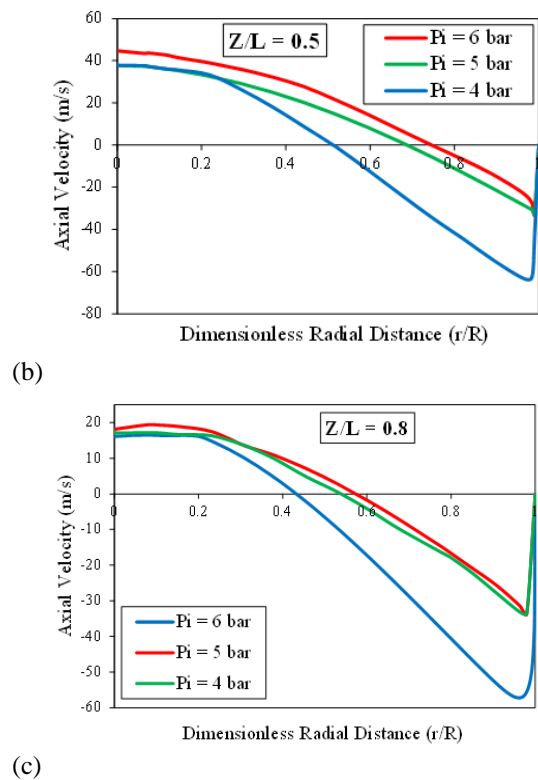


Fig. 14. Radial profiles of axial velocity at different axial locations

CONCLUSIONS

Various studies of the mechanism of separation of energy in the vortex tube from the last century had been presented but until now, there is no well-accepted demonstration for the physical analysis. The reason for non-understanding this phenomenon is a return to the fact of the complex internal flow. So, the aims of this investigation will be concentrated on the characteristics of the flow in the vortex tube and the performance. A new apparatus was designed experimentally and compared with CFD analysis. The dimensions of the experimental equipment have a total length of 104 mm and an inner diameter of 8 mm, made of stainless steel. The parameters were tested under three different inlet pressures (4, 5 and 6 bar) with inlet stagnation temperature of 293 K and the dimensionless cold mass fraction range (0.2-0.8). The numerical investigation was performed by using 3D CFD and a standard $k-\epsilon$ turbulence model using FLUENT software package. A good agreement was found between the experimental investigation and the CFD model with a deviation of less than or equal to 7%. ΔT_c increases with an increase of the cold mass fraction and the highest value occur at $\alpha = 0.3$. The data from the experimental study showed an increase of the inlet pressure causes increasing ΔT_c , where maximum value occurs at $P = 6$ bar. Two types of velocity were simulated (swirl and axial) with

different axial locations ranged (0.2-0.8), the results showed that the swirl velocity has the highest value. Finally, the power separation rate as a heat pump and a refrigerator was investigated and the results showed that it changed from 0.055 to 0.155 kW. The future research direction can be suggested as followings for other researchers:

1. Investigation of the vortex tube with different shapes and the number of nozzles on its performance.
2. Studying the effect of boundary layer formation along the tube.
3. Studying the current investigation with different gases and checking the ability of the vortex tube to separate a number of gasses into two outlet streams with different gas concentrations.
4. Development of the vortex tube by adding the effect of parameters (for example the effect of secondary circulation).
5. Investigation about the convergent-divergent angle to increase the energy separation.
6. Using two types of phases (gas and liquid) to understand the flow behavior.

REFERENCES

- Behera, U., Paul, P.J., Kasthuriengen, S., Karunanithi, R., Ram, S.N., Dinesh, K. and Jacob, S., "CFD analysis and experimental investigations towards optimizing the parameters of Ranque–Hilsch vortex tube," *Int. J. Heat Mass Transfer*, vol. 48, pp. 1961–1973 (2005).
- Dawoodian, M., Dadvand, A. and Hassanzadeh, A., "CFD and experimental analysis of drag coefficient and flow field's manner in a Parachute for various Reynolds numbers and different vent ratios," *ISRN Aerospace Eng.*, V. 20, Article ID 320563, 8 pages (2013).
- Kalal, M., Matas, R. and Linhart, J., "Experimental study and CFD analysis on vortex tube," *HEFAT, 6th International Conference on Heat Transfer, Fluid Mechanics and Thermodynamics*, Pretoria, South Africa (2008).
- Khodayari Babil, A. and Kim, J., "A Capillary Flow-Driven Microfluidic System for Microparticle-Labeled Immunoassay," *Analyst*, vol. 143, pp. 3335-3342 (2018).
- Kirmaci, V. and Kaya, H., "Effects of working fluid, nozzle number, nozzle material and connection type on the thermal performance of a Ranque–Hilsch vortex tube: A review," *Int. J. Refrig.*, vol. 91, pp. 254-266 (2018).
- Matveev, K.I. and Leachman, J., "Numerical investigation of vortex tubes with extended vortex chambers," *Int. J. Refrig.*, vol. 108, pp. 145-153 (2019).

- Pourmahmoud, N., Rashidzadeh, M. and Hassanzadeh, A., "CFD investigation of inlet pressure effects on the energy separation in a vortex tube with convergent nozzles," *Eng. Comput.*, vol.32, No.5, pp. 1323-1342 (2015a).
- Pourmahmoud, N., Esmaily, R. and Hassanzadeh, A., "Experimental Investigation of Diameter of Cold End Orifice Effect in Vortex Tube," *J. Thermopgys. and Heat Trans.*, vol. 29, No. 3, pp. 629-632 (2015a).
- Pourmahmoud, N., Jahangirami, A., Hassanzadeh, A. and Izadi S.A., "Numerical investigation of energy separation in a low pressure vortex tube under different axial angles of injection nozzles," *Modares Mech. Eng.*, vol. 13, No. 7, pp. 64-73 (in Persian) (2013).
- Pourmahmoud, N., Sepehrian Azar, S. and Hassanzadeh, A., "Numerical simulation of secondary vortex chamber effect on the cooling capacity enhancement of vortex tube," *Heat Mass Trans.*, vol.50, No. 9, pp. 1225-1236 (2014a).
- Pourmahmoud, N., Hassanzadeh, A. and Moutaby, O., "Numerical investigation of operating pressure effects on the performance of a vortex tube," *Therm. Sci.*, vol. 18, No. 2, pp. 507-520 (2014b).
- Promvong, P. and Eiamsa-ard, S., "Investigation on the vortex thermal separation in vortex tube refrigerator," *Sci. Asia*, vol. 31, pp. 215-223 (2005).
- Ranque, G.J., "Experiments on expansion in a vortex with simultaneous exhaust of hot air and cold air," *Le J. De Phys.*, vol. 4, pp. 1125-1130 (1933).
- Sadaghiyani, O.K., Boubakran, M.S. and Hassanzadeh, A., "Energy and exergy analysis of parabolic trough collectors," *Int. J. Heat and Tech.*, vol. 36, No. 1, pp. 147-158 (2018).
- Ye, A., Lijo, V., Setoguchi, T. and Kim, H.D., "An investigation of temperature separation phenomenon in the vortex chamber," *HEFAT, 10th Int. Conference on Heat Tran., Fluid Mech. and Thermodynamic.*, Florida, USA (2014).
- m total mass of vehicle
 Z Axial direction along the tube
 α Cold mass fraction
 ρ Density (kg.m^{-3})
 μ Dynamic viscosity ($\text{kg.m}^{-1}\text{s}^{-1}$)
 μ_t Turbulent viscosity ($\text{kg.m}^{-1}\text{s}^{-1}$)
 τ_{ij} Stress tensor components
 k turbulence kinetic energy
 ε rate of dissipation.
 \dot{Q} Energy (power) separation rate

NOMENCLATURE

- c Cold
 C_p Specific heat capacity in constant P
 D Diameter of vortex tube (mm)
 h Hot
 i Inlet
 L Length of vortex tube (mm)
 P Pressure ($Pascal$)
 T Temperature (K)
 \dot{m} mass flow rate